Geological Survey of Israel
Ministry of Energy

Recent seawater intrusion into deep aquifer determined by the radioactive noble-gas isotopes ^{81}Kr and ^{39}Ar

Yoseph Yechieli, Reika Yokochi, Michael Zilberbrand, Zheng-Tian Lu, Roland Purtschert, Jürgen Sueltenfuss, Wei Jiang, Jake Zappala, Peter Mueller, Ryan Bernier, Naama Avrahamov, Eilon Adar, Firas Talhami, Yakov Livshitz, Avihu Burg

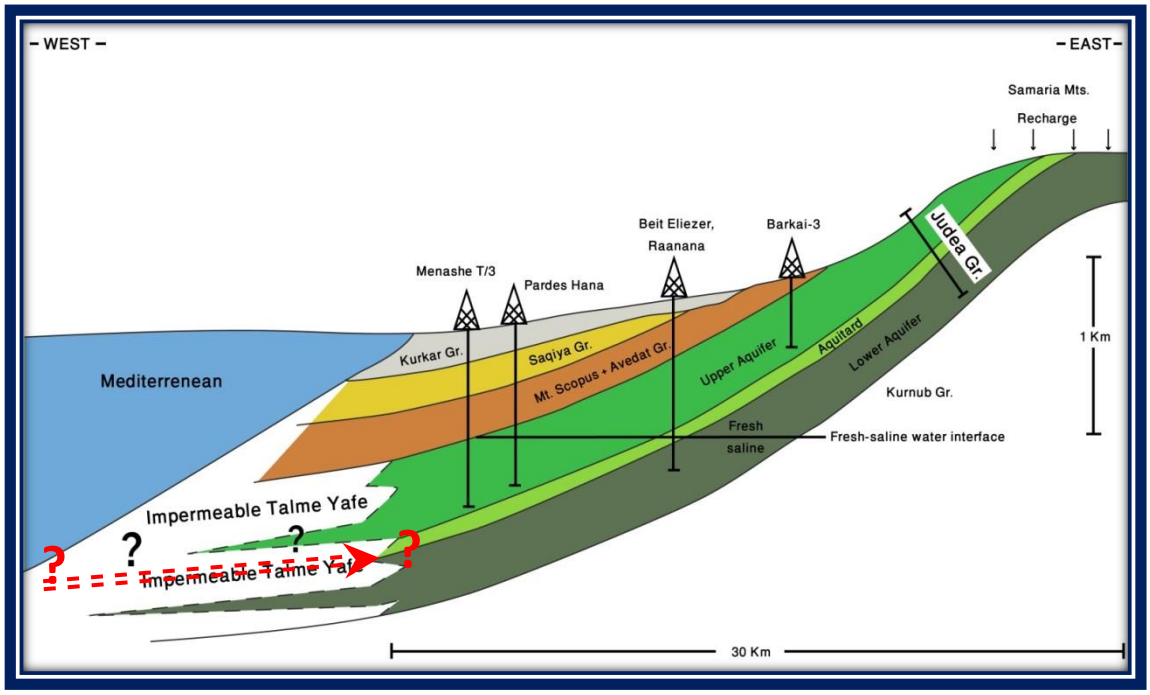

Report GSI/15/2018 Jerusalem, March 2018

Geological Survey of Israel
Ministry of Energy

Recent seawater intrusion into deep aquifer determined by the radioactive noble-gas isotopes ^{81}Kr and ^{39}Ar

Yoseph Yechieli[a,b*], Reika Yokochi[c], Michael Zilberbrand[d], Zheng-Tian Lu[e,f], Roland Purtschert[g], Jürgen Sueltenfuss[h], Wei Jiang[e,f], Jake Zappala[c,e], Peter Mueller[e], Ryan Bernier[c], Naama Avrahamov[i], Eilon Adar[b], Firas Talhami[d], Yakov Livshitz[d], Avihu Burg[a]

[a]Geological Survey of Israel, 30 Malkei Israel St., Jerusalem 9550161, Israel
[b]Zuckerberg Institute for Water Research, Ben-Gurion University, Sede Boqer Campus, 8499000, Israel
[c]Department of the Geophysical Sciences, The University of Chicago, IL, USA
[d]Hydrological Service, 50 Yirmeyahu St, Jerusalem, Israel
[e]Physics Division, Argonne National Laboratory, Argonne, IL 60439, USA
[f]CAS Center for Excellence in Quantum Information and Quantum Physics, University of Science and Technology of China, Hefei, Anhui 230026, China
[g]Climate and Environmental Physics, Physics Institute and the Oeschger Centre for Climate Change Research, University of Bern, Sidlerstrasse 5, 3012 Bern, Switzerland

[h]Institute of Environmental Physics, Section of Oceanography, University of Bremen, Otto Hahn Allee 1, Bremen, 28359, Germany
[i]Eastern R&D Center, Ariel, Science Park, 40700, Israel

Report GSI/15/2018 Jerusalem, March 2018

Abstract

Radioactive noble-gas isotopes tracers ^{81}Kr and ^{39}Ar are used to measure for the first time the residence times of deep (~1000 m) saline coastal groundwater, and to determine the current connection mode with the sea. These tracers allowed the estimation of the average rate of seawater intrusion into this deep aquifer in Israel, located near the Mediterranean Sea. ^{81}Kr-ages of the saline water samples are younger than 40 ka, clearly contradicting previously estimated ages of up to several million years based on scarce hydrogeological considerations. The new results imply a stronger and more recent connection between the aquifer and the sea, and indicate that the intrusion occurred during the sea-level rise that began about 20 ka ago. These coastal aquifers need to be managed with caution because lowering of the adjacent fresh water level due to over pumping could accelerate seawater intrusion in a relatively short time. This study demonstrates the suitability of these two noble-gas tracers for the examination of hydrogeological systems in general and for the study of seawater intrusion in particular.

Introduction

Coastal aquifers are potentially prone to salinization from multiple sources, including dissolution of subsurface evaporates, ancient trapped seawater, and ongoing seawater intrusion. The issue of coastal aquifer degradation has become increasingly acute in the past few decades due to over pumping that induces saline water into adjacent freshwater aquifers. In most cases, seawater intrusion rates are inferred from increase in salinity (Acworth and Dasey, 2003; Linderfelt and Turner, 2001), change of chemical composition (Russak et al, 2016; Mercado, 1985), or movement of the fresh-saline water interface (Melloul and Zeitoun, 1999). Direct determination of the seawater intrusion rate was previously done, based only on radiocarbon and tritium tracers (Sivan et al, 2005; Yechieli et al, 2001; Yechieli et al, 2009). However, the interpretation of radiocarbon results is complicated by water-rock interactions (Mook, 1980), and dating by tritium became ambiguous due to the low values in recent precipitation and its short half-life. Moreover, saline well water usually mixes with fresh water, further complicating the chronological interpretation. Noble-gas radionuclides, with chemical inertness, simple source function, and limited subsurface production, are thus emerging as ideal tracers of groundwater movement. Indeed, dating of fresh groundwater with noble gases has recently been performed in many parts of the world, using ^{85}Kr (half life of 10.7 a) and ^{3}He (which is decaying from ^{3}H, whose half life is 12.4 a) for short-term hydrological processes (Althaus et al, 2009; Visser et al, 2013), ^{39}Ar (269 a) for intermediate, and ^{81}Kr (229 ka) for long-term processes (Gerber et al, 2017; Aggarwal et al, 2015). Prior to the current work, groundwater with salinity close to that of seawater (> 75% seawater) has not been dated by noble-gas radionuclides.

Site description

The Yarkon-Taninim Basin (YTB) of Israel is the western portion of the regional Upper Cretaceous Mountain aquifer. The basin stretches over 10,500 km^2, from the water divide in the Judea and Samaria mountains in the east to the Mediterranean coast in the west (Figure 1). The northern border of the basin extends to the Yizrael Valley, Mount Carmel, and to the Taninim spring. The southern border extends into the Sinai Peninsula in Egypt and to the northern Negev desert (Goldshtoff et al, 1980; Shachnai, 1980; Weinberger et al, 1994; Dafny et al, 2010). Precipitation in most of the YTB drainage basin is about 550 mm/year, all occurring in winter Mediterranean rain events, and the recharge coefficient is 30-33% (Dafny et al, 2010; Guttman and Zukerman 1995).

The major hydrogeological unit of the YTB is the Judea Group built of 600-900 m thick Upper Cretaceous karstic limestones and dolomites with some marls and chalks. The aquifer is divided into upper and lower sub-aquifers by a leaky marly aquitard. The units in the aquifer are continuous throughout the entire basin and generally dip to the west. In the eastern areas (Judea and Samaria mountains), the aquifer is exposed and directly replenished by rainfall (Figure 2). Westwards, the aquifer becomes confined under relatively thick impermeable chalks and marls of the Senonian Mount Scopus Group and the Eocene Avedat Group. The phreatic parts of the aquifer, as well as the eastern confined part, contain mostly high-quality young groundwater. A gradual lateral lithological transition from the karstic permeable Judea Group rocks to the mainly argillaceous and impermeable Talme Yafe facies (Figure 2) occurs at the western margins of the basin, mostly along the Mediterranean shoreline (Bein, 1974). This impermeable unit was assumed to act as a bidirectional hydrological barrier between the Mediterranean Sea and the Judea Group aquifer, preventing flow toward the sea. This results in northward flow of the fresh water within the confined part of the aquifer towards the two natural outlets: the Yarkon springs in the central part of the basin and the Taninim springs at its northern tip (Figure 1).

This main and long S-N flow trajectory is fed all along by recharge water that joins the main trajectory from the east (Figure 1).

The northwestern confined portion of the YTB, north of the city of Netanya, contains saline groundwater (Rosenthal et al, 1999) (Figure1). In this area, an unusual sharp and almost horizontal interface between saline and fresh water was recognized in deep monitoring boreholes (Figure 2). The salinity and chemical composition of this saline water resembles that of the Mediterranean Sea (Cl~22,000 mg/l), while always containing also a small fraction of fresh water of Cl~100 mg/l (at least 10%). Because of the impermeable nature of the Talme Yafe facies, a current hydraulic disconnection to the Mediterranean Sea was assumed, and Neogene trapped seawater (age of several millions years) origin of the salinity in the northwestern part of the aquifer has long been postulated (Rosenthal et al, 1999; Bein and Burg, 2001). In the Neogene, the impermeable clayey Yafo Formation was deposited, which could explain the confinement of this saline water body. However, it should be noted that few hydrological studies suggested current seawater intrusion either directly or along a main fault zone at the northern tip of the basin (Kafri and Arad, 1979; Paster et al, 2006).

In this work, ^{81}Kr and ^{39}Ar tracers were employed for the first time to determine the time scale of the seawater penetration into an adjacent aquifer. These tracers can serve as a diagnostic tool for distinguishing between trapped saline water of Neogene age and active, current seawater intrusion from the Mediterranean Sea. In particular, the results are essential for estimating the degree of connection between the sea and any nearby active and exploited aquifers, and for minimizing salinization of such coastal aquifers.

Materials and Methods

Field sampling and measurements.

Five deep boreholes in the saline part of the western mountain aquifer of YTB (Figure 1) were sampled for chemical analysis of major ions, stable isotopes of oxygen and hydrogen, ^{81}Kr, and other noble gases: two in June 2014 and three in November 2015. Technical details, such as depths of boreholes and intervals of screens, are given in Table 1. Additional samples for ^{39}Ar and ^{14}C analyses were collected in the 2015 campaign. Onsite measurements of pH, dissolved O_2, water temperature and electrical conductivity were carried out. Two to five cubic meters of groundwater were degassed in the field for radioactive noble gases ^{39}Ar, ^{81}Kr and ^{85}Kr according to the procedure described by Purtschert et al (2013) and Yokochi (2016).

Composition of major ions and stable isotopes were determined according to standard methods in the laboratories at the Geological Survey of Israel (GSI). The isotopic results of $\delta^{18}O$ and δD are reported on the SMOW scale and the precision of the measurement is ±0.1‰ and ±1‰, respectively. Radiocarbon samples were collected in 200-ml dark sealed glass and measured in the AMS Laboratory, New Zealand. The activities are expressed as a percentage of modern carbon (pMC). The $\delta^{13}C$ contents were measured in both AMS and GSI Laboratories, and are expressed in permil variations from the Vienna Peedee Belemnite Standard (% VPDB). Analyses of ^{3}H, He isotopes and Ne were conducted at the noble gas laboratory of the Institute of Environmental Physics, University of Bremen. For the He and Ne analysis, bulk water samples collected in 40-ml copper tubes sealed with pinch-off clamps, were degassed and cryogenically separated for the analyses by a quadrupole mass spectrometer (Balzers QMG112A) and a high-resolution sector-field mass spectrometer (MAP 215-50). For groundwater samples, the precision of the He and Ne concentrations is better than 1% and for the $^{3}He/^{4}He$ ratio better than 0.5%. ^{3}H was analyzed with the ^{3}He-ingrowth method (Clarke et al, 1976;

Sültenfuß et al, 2009) with a precision of ~0.03TU: 500 g of water were degassed and stored for the accumulation of the ^{3}H decay product (^{3}He) in dedicated He-free glass bulbs. After a storage period of 2-3 months, ^{3}He was analyzed with a mass spectrometric system.

Separation and purification of krypton and argon from the bulk gas were done in the laboratories of both the University of Chicago and University of Bern using cryogenic absorption and gas chromatography (Purtschert et al, 2013; Yokochi, 2016; Riedmann and Purtschert 2016). Later, $^{81}Kr/Kr$ and $^{85}Kr/Kr$ were measured using the Atom Trap Trace Analysis (ATTA) method (Lu et al, 2013; Jiang et al, 2012; Chen et al, 1999) in the Laboratory for Radiokrypton Dating, Argonne National Laboratory, USA. At least 10 μL STP of Kr gas sample is required for measurement. The ^{81}Kr partial modern values are reported with 1-sigma uncertainty. Partial modern values which exceed the modern atmospheric value defined as due to statistical fluctuations of the ^{81}Kr atom count would represent unphysical groundwater ages of less than zero. In these cases, we redistribute the groundwater age probabilities into the physical range following the unified approach method (Feldman and Cousins, 1998) and obtain ^{81}Kr-age limits with a confidence level of 90%. The ^{39}Ar activities were measured by low-level gas proportional counting in the Deep Laboratory of the Physics Institute, University of Bern (Loosli, 1983; Loosli et al, 1986; Forster et al, 1992; Riedmann and Purtschert 2016).

Relevant processes for data interpretation.

All samples discussed here contain both fresh and saline water components, each with its distinct flow path and residence time. Henceforth, we define age for each component as the time since penetration or recharge of the water into the aquifer. When discussing the saline water, the age (or residence time) is considered to be from the time of penetration of the seawater into the bottom sediment (Yechieli et al, 2009). In such a case, there are three relevant processes: (1) long term

seawater intrusion due to natural density-driven circulation near the sea shore; (2) the effect of sea level rise; (3) seawater encroachment landwards due to the short term effect of pumping. The rate of seawater intrusion, and therefore the age of the saline water, would be the result of the superposition of these three possible processes. The initial values of the penetrating seawater can be assumed to be similar to the current ones since the age of the bottom Mediterranean Sea water is probably not more than ~100 years according to their radiocarbon values (Broecker and Gerard, 1969). The age of the fresh water component is determined as the time since recharge into the subsurface, where the water loses its contact with the atmosphere, down to the sampling point.

The interpretation of the ages concluded from two of the noble gases concentrations (^{81}Kr, ^{39}Ar - half-life of 229 ka and 269 years, respectively) is relatively simple since they do not chemically interact with the aquifer's rock and therefore do not require specific corrections for chemical processes (as is the case of ^{14}C, see below). However, physical processes such as diffusive exchange with stagnant water bodies (all tracers, Sanford, 1997) or nucleonic production due to neutron activation of potassium for ^{39}Ar may affect the tracers' concentrations (Lehmann et al, 1993; Purtschert et al, 2004). Practically, diffusion is more pronounced for tracers with longer half-life (e.g. ^{14}C) than for fast decaying tracers. The latter (^{39}Ar) does not ''see'' the total inactive system volume since the time to diffusively reach the inactive volume is much longer than the mean lifetime of the tracer. Therefore, ^{14}C (half-life of 5730 years) is more sensitive to the diffusion process than is ^{39}Ar (half-life of 269 years) resulting in an apparent overestimation of ^{14}C ages compared to ^{39}Ar ages (Mayer et al, 2014). ^{81}Kr ages are similarly affected by this process despite the slightly reduced diffusion coefficient due to the larger mass of the Kr atom. Uncorrected ^{81}Kr ages therefore represent upper age limits if diffusive exchange is neglected.

Moreover, the translation of radiocarbon activities into ages could also be complicated and inconclusive due to chemical processes, such as water-rock interaction and isotopic exchange (Mook, 1980; Gonfiantini and Zuppi, 2013). Thus, dating by ^{14}C is carried out with the aid of mass balance equations, using computer codes such as the Netpath and PhreeqC, which take into account the known chemical reactions. These codes estimate one age for any mixed sample (the obtained saline water sample in our case) and do not provide the distinct age of each component in the mixed sample. Since seawater is the larger component in our mixtures, the obtained ages are regarded as a reasonable approximation. An estimated initial value of 60 pMC can be assumed for many cases, also according to the finding in the nearby coastal aquifer, mainly due to oxidation of old organic matter in the seawater component (Sivan et al, 2005), and due to chemical processes in the unsaturated zone in the fresh water component (e.g. Carmi et al, 2007).

The effect of diffusive exchange between young water in permeable units and old groundwater in less permeable units can increase the apparent radiocarbon age by ~50% in the case of granular aquiferic section separated by clayey impermeable layers and/or when the volume ratio between fractures and rock matrix is relatively low (Sanford, 1997). In the YTB there are indeed less permeable marly units in the karstic carbonate Judea Group aquifer but water and solute can exchange between the karstic channels characterized by very fast water flow and the surrounding porous massive rocks with almost stagnant pore water. The high degree of heterogeneity of the karstic system can lead to a highly dispersive flow and thus wide age distributions (Ghasemizadeh et al, 2012).

Results and discussion

The results of all dating tracers are summarized, along with other chemical parameters, in Table 1. The concentration of ^{85}Kr in all gas samples are below the detection limit of ~ 0.5 dpm/ccKr (less

than 1% of the current atmospheric concentration of 82 dpm/ccKr). This has two implications: first, contamination of the samples by ambient air during sampling is minimal. Therefore, no correction for air contamination is needed for the ^{81}Kr and ^{39}Ar concentrations. Second, all waters are older than ~ 50 years, thus the contribution of young water component is at most relatively small. The almost negligible ^{3}H concentrations in Raanana Deep (RD) and Taninim 7 (T7) wells (0.05 TU, compared to ~ 3.5 TU in modern precipitation) are in good agreement with this observation. For Bet Eliezer (BE) well, however, the measured value of ^{3}H of 0.36 TU is significantly above the detection limit, indicating the presence of about 10% young water from the period of 1960-1985, when ^{3}H/^{85}Kr ratios in the Earth's surface water were much higher. Yet, ^{3}H-^{3}He ages could not be calculated for these three samples since the He isotopes and Ne results display a mixture of large crustal and mantle He sources. Ne concentrations are near equilibrium concentrations of saltwater. ^{4}He concentrations are not in contradiction to ^{39}Ar and ^{81}Kr. The almost modern ^{81}Kr activities in all measured samples (Table 1) consistently indicate short water residence time. The lowest value was measured in BE (0.94), indicating an upper age limit of 40 ka. The relatively low ^{39}Ar activities (< 27%) points to a component that is older than several hundred years.

All three ^{14}C samples (T7, RD, BE) have low radiocarbon contents (2.9, 3.6 and 5.3 pMC, respectively). Other YTB saline groundwater samples previously analyzed (Burg et al, 2006; Burg and Talhami, 2013) also presented low ^{14}C activities, with an inverse correlation between ^{14}C and salinity (Figure 3), suggesting that the fresh water component is much younger than the saline water. The values of δ^{18}O and δD in the more saline samples are close to that of current seawater and plot on a seawater-freshwater mixing line (Figure 4). Accordingly, all samples discussed here are considered as containing different degrees of mixture of seawater and freshwater.

Residence times of mixed groundwater components.

The saline groundwater in the study area is a mixture of fresh groundwater from the east (and south) and seawater that intruded from the west. The proportion of mixing was determined by assuming Cl ~ 22.5 g/L for the seawater end member. The fresh water contribution (y) in the above three samples are in the range of 9-17%. Concentrations of Ar and Kr in the fresh and seawater component are estimated based on the recharge conditions of both water components: For seawater a recharge elevation of 0 m and salinity of 39‰ and for the freshwater a recharge altitude of 400 meters and a salinity of 0‰ were assumed. No excess air was considered for both water components. Because of the reduced solubility of Ar and Kr in seawater, both gases are depleted in the seawater compared to freshwater with a depletion factor D of 0.82 (Weiss, 1971; Weiss and Kyser, 1978). The weighted Ar and Kr contributions in the freshwater ($E=E_{Ar}=E_{Kr}$) are then given by: $E = y/(y+(1-y)D)$. For ^{39}Ar, the possibility of underground production (Purtschert and Althaus, 2012) also needs to be considered. The lowest measured value of 10% modern at Taninim 7 can be regarded as an upper limit on the secular equilibrium concentration (P) due to underground production. Therefore, a range of 0-10% modern is assumed for all samples and for both the sea and the fresh water components. This is justified by the fact that both components were sampled from the same formation, which is built of shallow marine carbonate of relatively uniform composition over a large area.

With the above calculated mixing proportions of Ar and Kr and the measured concentrations of ^{39}Ar and ^{81}Kr, the following activity budget can be formulated in eq 1:

$$^{39}Ar_m = E_{Ar} \cdot \left((\mathrm{A}_0 - P) \cdot \exp(-\lambda_{Ar} \cdot t_f) + \mathrm{P}\right) + (1 - E_{Ar}) \cdot \left((\mathrm{A}_0 - P) \cdot \exp(-\lambda_{Ar} \cdot t_s) + \mathrm{P}\right) \quad (1a)$$

$$^{81}Kr_m = E_{Kr} \cdot Kr_0 \cdot \exp(-\lambda_{Kr} \cdot t_f) + (1 - E_{Kr}) \cdot Kr_0 \exp(-\lambda_{Kr} \cdot t_s) \quad (1b)$$

Underground production is described as an ingrowth process as function of groundwater residence time and the decay constant of ^{39}Ar. Here, the subscript *m* refers to the measured tracer concentrations, λ*'s* are the decay constants, and t_f and t_s are the ages of the fresh and saline water components, respectively. Equations (1a) and (1b) must be fulfilled for any valid pairs of t_f and t_s in consideration of the analytical uncertainties and the possible range of underground production (P) of ^{39}Ar.

The multi-tracer chronological constraints are depicted in Figure 5 a-c. Each tracer defines a band bound by the uncertainty of observed value on the t_f - t_s plane. For ^{39}Ar, two bands are shown for the two extreme cases of subsurface productions - 0 and 10% modern. For $t_f < t_s$, the upper bound of saline water age is set by the lower limit of ^{81}Kr data shown as grey curves, and encompasses young age, possibly as young as a few hundred years according to the lower age limit set by ^{39}Ar. This is not really true for the BE sample which is located farthest from the coast and closest to the current recharge zone in the mountain area. The age of the saline component in this well is 13-40 ka (Table 2), whereas the elevated ^{3}H/^{85}Kr ratio indicates that the recharge of the fresh component was closer to the peak of the atmospheric bomb tests period (1960-1985). This well exhibits the youngest freshwater component (highest ^{39}Ar activity) and the oldest saline water component (lowest ^{81}Kr activity) of all wells implying the possibility of active seawater intrusion from the west. The ages of the fresh water component in the other two samples (RD and T7) are limited by the absence of ^{3}H and ^{85}Kr on the lower end, and the boundary condition $t_f < t_s$ on the upper limit. The age of the saline component in these samples is younger than 13 ka according to the ^{81}Kr activity.

Implications of radiocarbon signatures.

An activity budget similar to the above eq (1b) can be formulated for ^{14}C in eq 2:

$$^{14}C_m = E_C \cdot C_0 \cdot \exp(-\lambda_C \cdot t_f) + (1 - E_C) \cdot C_0 \exp(-\lambda_C \cdot t_s) \quad (2)$$

The following assumptions are taken into account: (1) an initial activity of 60 pMC; (2) the above described mixing proportion; (3) an enrichment factor of ~2 (DIC of freshwater is twice higher compared to saline water (Burg and Talhami, 2013), and (4) the ages of the fresh and saline water component deduced above. Accordingly, the calculated ^{14}C activities are 18, 20 and 15 pMC for BE, RD and T7, respectively. These values are much higher than those measured in the range of 2.9 - 5.3 pMC (Table 1). Groundwater dating using ^{14}C in the present case, therefore, has to be done with caution. Meanwhile, the $\delta^{13}C$ values of the saline water component are lighter than those of the current seawater, indicating the effect of oxidation of organic matter of seafloor sediments, containing dead carbon during the seawater penetration (similar to the process in the shallow coastal aquifer; Sivan et al, 2005). Entering both the ^{14}C activities and $\delta^{13}C$ values into PhreeqC or Netpath geochemical codes led to adjusted residence time of 21 - 27 ka for the saline water of the YTB (Table S2). The apparent difference between the relatively old apparent radiocarbon ages, and the ages deduced from the ^{39}Ar and ^{81}Kr dating methods, can be explained by several chemical (water-rock interaction, e.g. Mook, 1980) and physical (matrix diffusion, Sanford, 1997) processes.

Our data can be used to constrain not only the time of seawater intrusion but also the residence time of the fresh groundwater (constituting 9-17% of the samples). Since HCO_3 in most fresh water samples is about twice that of seawater, the contribution of carbon from the fresh water could be up to 18-34% of the total. At such mixing ratios, the radiocarbon of the fresh groundwater component has to be 9-30 pMC in the three samples or even less for other samples (Figure 3; Table S1), even if we take the seawater component to be close to 0 pMC (which is probably too low a value according to the ^{81}Kr data).

Regarding the BE sample, with its relatively high ^{39}Ar and ^{3}H, there is an unexpected contradiction between the relatively old radiocarbon ages (several thousands of years, 16-30 pMC;

Table S1) and the young ^{39}Ar ages (several hundreds of years, >0.27, Table 1) of the fresh component. Pronounced mixing of the water components with different ages, as expected in a karstic system, is a process that may explain this discrepancy because of the concave exponential decay curve and the shorter half-life of ^{39}Ar compared to ^{14}C. Yet, details of the mixing process cannot be resolved with the restricted available data. It is suggested that the discrepancy could be due to dispersive mixing of several fresh water bodies of different ages and flow rates. The youngest could be the component that percolates into the Samaria Mountains in the east while the oldest could be the water body that moves slower at the fresh-saline water interface zone or the component that flows from the farther southern part of the aquifer (Dafny et al, 2010). The mixing of these components is probably due to natural flow near the interface zone.

Loss of ^{14}C from the groundwater into the surrounding aquifer matrix is another process that could lead to much older apparent ^{14}C ages (Sanford, 1997). This process would also affect ^{39}Ar and ^{81}Kr but to different extent as a function of half-life, diffusion coefficients and geometry and spacing of permeable and stagnant zones. This process can explain at least part of the above contradiction in the ages of the BE sample. By assuming similar conditions for the intruding seawater, and similar diffusion with old connate water during the inland intrusion, the age can be reduced by ~50%.[30] In accordance, the age of the saline water would be younger than that discussed above by ~50% (~10 ka instead of ~20 ka).

Other age constraints.

More constraints on the age of the saline water can be derived from the isotopic signature. According to the mixing line (Figure 4a), the isotopic signature of the old, sea water component is quite similar to that of the present seawater (e.g. $\delta^{18}O$ of ~1.5‰ and 1.8‰ in old and recent seawater, respectively). δD values (Figure 4b) of the old saline water end-member are also similar to that of the current seawater. On the other hand, the isotopic values during the period of 15-120 ka were different from the present ones by ~2‰. This implies that the intrusion took place in sea conditions similar to those of the last 15 ka, following the most recent sea level rise after the last glacial period, or in previous high sea level periods in the Pleistocene (~120 ka ago). Only the former scenario is in accordance with the ^{81}Kr data (Figure 5).

Taking into account all the above age results and analyses, it can be summarized that the intruding seawater is of Holocene age, except the BE sample farther away from the coast showing late Pleistocene age. The intrusion may have been mainly during the last sea level rise or continuous since then.

Hydrological implication.

The much younger than expected ages of the saline groundwater suggest an active hydraulic connection between the Judea Group aquifer and the Mediterranean Sea. There are two primary hypotheses for the location of this recent penetration (Paster et al, 2006; Dafny, 2009). First is from the northern part of the YTB going southward, either from Or Akiva fault or from the submarine exposure of this aquifer. The second option is through several hydraulic openings in the impermeable marly Talme Yafe facies, either due to lithological changes or through faults or buried erosional channels filled with coarse-grained sediments with higher permeability. The first hypothesis would result in age

gradient from north to south, which was not found in the five ^{81}Kr ages that were obtained in this study. The second hypothesis anticipates increasing seawater residence time with distance from the sea, the indication for this being the oldest age of the BE sample farthest from the coast.

The average rate of seawater intrusion may be estimated from the subsurface residence times. As discussed above, this rate would be superposition of three processes: the natural circulation of seawater in the aquifer, the increased rate due to the rapid rise of sea level in the beginning of the Holocene and effects of over pumping. The effect of sea level rise is expected to be especially significant due to the increase in hydraulic gradient when the sea level rose by 120 m in a relatively short time (Morrissey et al, 2010). Thus, the intrusion of seawater could have occurred over a much shorter time at the transition to the Holocene and could be less active today. However, since the above three processes cannot be separated, the estimation of the rate of intrusion is an average value for the entire distance from the sea to the sampled wells and ignores heterogeneity in this rate. Accordingly, assuming that the flow is from the west to the east and the distance from the contact zone of the aquifer with the sea to the sampled wells is ~20-30 km (Figure 2), and the ages of saline water are about 10 ka, a rough estimation of the average rate of seawater intrusion into the aquifer yields a value of about 2-3 m/year. It is interesting to note that this value is quite similar to a previous estimate in the coastal aquifer of Israel based on geochemical tracers (Sivan et al, 2005), despite the difference in lithology and hydrological conditions.

The most important aspect of these results is that the saline water is not Neogenic seawater trapped in isolated pockets in the aquifer. Instead, the young ages and the aging inland imply active, current, hydraulic connectivity between the aquifer and the Mediterranean Sea. Moreover, and from a practical aspect, if the saline water was identified as old, it could be considered to contain finite volume of storage. The opposite is true if the age is young and the seawater mass in the aquifer is

connected to the current sea. In the former case, pumping of the old saline water may be conducted in order to use this water for desalination and decrease the potential risk of this problematic water i.e. increase salinity of the fresh water volume. Such action will have no chance of success in the case of connection with the sea since the water head is permanent and stable (sea level) regardless of the rate of pumping. Consequently, according to our findings over-pumping of fresh water in the eastern confined portion of the YTB would draw more saline water from the infinite reservoir of Mediterranean Sea. This important water resource needs to be managed accordingly in order to sustain its quality. Moreover, the fresh-saline water interface may rise in the future in response to the anticipated sea level rise.

Summary and conclusions

This work demonstrates that noble gas radionuclides are ideal tracers for determining the rate of seawater intrusion. The multi-tracer approach of these relatively more reliable isotopes provides effective assessments of age structures for both seawater and fresh water components that mixed in the coastal aquifer. Having such new tools will encourage more similar hydrogeological studies in which new drillings and dating of coastal saline groundwater will enable determination of the connection between the sea and the adjacent aquifer and estimation of the risk of seawater intrusion.

Our results change previous perception and indicate that the age of the saline water in the western part of the aquifer is relatively young, and its origin is from active seawater intrusion that entered the deep confined portion of the aquifer during the Holocene. These young ages imply that pumping of fresh water should be carefully managed due to the risk of salinization by accelerated seawater intrusion, and that the fresh-saline water interface may rise in response to the anticipated sea level rise.

Acknowledgements

Haim Hemo and Iyad Swaed are thanked for their help in field sampling and Roi Ram for helping in data collection and organization. Hana Netzer and Batsheva Cohen from the graphic department (GSI) are thanked for their technical help. We thank the Israel Water Authority and the BSF for funding this project through grant number 2014351. W.J., Z.-T.L., P.M., J.C.Z. and the Laboratory for Radiokrypton Dating at Argonne are supported by DOE, Office of Nuclear Physics, under contract DE-AC02-06CH11357.

References

Acworth, R. I.; Dasey, G. R. 2003. Mapping of the hyporheic zone around a tidal creek using a combination of borehole logging, borehole electrical tomography and cross-creek electrical imaging, New South Wales, Australia. *Hydrogeology Journal*, *11* (3), 368-377.

Aggarwal, P. K.; Matsumoto, T.; Sturchio, N. C.; Chang, H. K.; Gastmans, D.; Araguas-Araguas, L. J.; Jiang, W.; Lu, Z-T,; Mueller, P.; Yokochi, R.; Purtschert, R.; Torgersen, T. 2015. Continental degassing of 4He by surficial discharge of deep groundwater. *Nature Geoscience***,** *8*, 35-39.

Althaus, R.; Klump, S.; Omnis, A.; Purtschert, R.; Kipfer, R.; Stauffer, F.; Kinzelbach, W. 2009. Noble gas tracers for characterisation of flow dynamics and origin of groundwater: A case study in Switzerland. *Journal of Hydrology*, *370*, 64-72.

Bein, A. 1974. Reef development at the Judea Group Rocks in the Carmel and in the Israeli coast. Ph.D Dissertation, The Hebrew University, Jerusalem, Israel, (in Hebrew, English Abstract).

Bein, A.; Burg, A. 2001. Quantitative, 3-D hydrogeological model for the Yarkon-Tanninim aquifer as a tool for assessment of operational limitation ("red lines") and planning of optimal exploitation, opening report; Rep GSI/28/2001; Geol. Surv. Isr., Jerusalem, Israel, (in Hebrew).

Broecker, W S; Gerard, R. 1969. Natural radiocarbon in the Mediterrranean Sea. *Limnology and Oceanography*, *14* (6), 883-888.

Burg, A.; Gavrieli, I.; Bein, A.; Fridman V. 2006. *The Yarkon-Taninim aquifer monitoring project; chemical and isotopic compositions in new monitoring wells and other selected wells. Final report*; Rep. GSI/26/2005; (in Hebrew).

Burg, A.; Talhami, F. 2013. *The Yarkon-Taninim aqu,ifer monitoring project; chemical and isotopic compositions in new monitoring wells and other selected wells, seventh year report*. Rep. GSI/7/2013. (Geol. Surv. Isr., Jerusalem; (in Hebrew).

Carmi, I.; Kronfeld, J.; Yechieli, Y.; Yakir, D.; Stiller, M.; Boaretto, E. 2007. Quantitative extraction of dissolved inorganic carbon (as CO2) and water by vacuum distillation from sediments of the unsaturated zone for carbon isotope analysis (13C and 14C). *Radiocarbon*, *49* (1), 83-94.

Chen, C. Y.; Li, Y. M.; Bailey, K.; O'Connor, T. P.; Young, L.; Lu, Z-T. 1999. Ultrasensitive isotope trace analyses with a magneto-optical trap. *Science* **,** *286*, 1139.

Clarke, W. B.; Jenkins, W. J.; Top, Z. 1976. Determination of tritium by mass spectrometric measurement of ^{3}He. *The International Journal of Applied Radiation and Isotopes* **,** *27*, 515-522.

Dafny, E. 2009. Groundwater Flow and Solute Transport within the Yarqon-Tanninim Aquifer, Israel. Ph.D. Dissertation, Hebrew University, Jerusalem, in Hebrew, English Abstract.

Dafny, E.; Burg, A.; Gvirtzman, H. 2010. Effects of karst and geological structure on groundwater flow: the case of Yarkon-Taninim aquifer. Israel. *J. Hydrology* **,** *389*, 260-275.

Feldman, G.; Cousins, R. D. 1998. Unified approach to the classical statistical analysis of small signals. *Phys. Rev. D.* **,** *57*, 3873.

Forster, M.; Maier, P.; Loosli, H. H. 1992 . Current techniques for measuring the activity of 37Ar and 39Ar in the environment. In *Isotopes of Noble Gases as Tracers in Environmental Studies*; IAEA, Vienna; pp 63–72.

Gerber, C.; Vaikmäe, R.; Aeschbach, W.; Babre, A.; Jiang, W.; Leuenberger, M.; Lu, Z-T.; Mokrik, R.; Müller, P.; Raidla, V.; Saks, T.; Waber, H. N.; Weissbach, T.; Zappala, J. C.; Purtschert, R. 2017. Using 81Kr and noble gases to characterize and date groundwater and brines in the Baltic Artesian Basin on the one-million-year timescale. *Geochimica et Cosmochimica Acta***,** *205*, 187-210.

Ghasemizadeh, R.; Hellwege, Fr,; Butscher, C.; Padilla, I.; Vesper, D.; Field, M.; Alshawabkeh A. 2012. Review: Groundwater flow and transport modeling of karst aquifers, with particular reference to the North Coast Limestone aquifer system of Puerto Rico. *Hydrogeol J.***,** *20* (8), 1441–1461.

Goldshtoff, Y.; Shachnai, E. 1980. *Yarqon-Taninim-Be'er Sheva basin. Setting and calibrating numerical model;* Rep. 01/80/58; Tahal Ltd., Tel Aviv, Israel; (in Hebrew).

Gonfiantini, R.; Zuppi, G. M. 2003. Carbon isotope exchange rate of DIC in karst groundwater. *Chemical Geology***,** *197*, 319-336.

Guttman, J.; Zukerman, H. 1995. Yarqon-Taninim – Beer Sheva groundwater basin: setting and calibrating flow model; Rep. 01/95/72; Tahal Ltd., Tel Aviv, Israel, (in Hebrew).

Jiang, W.; Bailey, K.; Lu, Z-T.; Mueller, P.; O'Connor, T. P.; Cheng, C-F.; Hu, S-M.; Purtschert, R.; Sturchio, N. C.; Sun, Y. R.; Williams, W. D.; Yang, G-M. 2012. An atom counter for measuring 81Kr and 85Kr in environmental samples *Geochimica et Cosmochimica Acta* **,** *91*, 1-6.

Kafri, U.; Arad, A. 1979. Current subsurface intrusion of Mediterranean seawater – a possible source of groundwater salinity in the Rift Valley System. *Israel. J. Hydrology* **,** *44*, 267-287.

Lehmann, B.; Davis, S.; Fabryka, M. J. 1993. Atmospheric and subsurface sources of stable and radioactive nuclides used for groundwater dating. *Water Resources Research***,** *29*, 2027-2040.

Linderfelt, W. R.; Turner, J. V. 2001. Interaction between shallow groundwater, saline surface water and nutrient discharge in a seasonal estuary: The Swan-Canning System: Special Issue: Integrating Research and Management for an Urban Estuarine System: The Swan - Canning Estuary, Western Australia. *Hydrological Processes, 15* (13), 2631-2653.

Loosli, H. H. 1983. A dating method with Argon-39. *Earth Planet. Sci. Lett.***,** *63*, 51-62.

Loosli, H. H.; Moell, M.; Oeschger, H.; Schotterer, U. 1986. Ten years of low level counting in the underground laboratory in Bern, Switzerland. *Nuclear Instr. Methods* **,** *B17*, 402-405.

Lu, Z-T.; Schlosser, P.; Smethie Jr., W. M.; Sturchio, N. C.; Fischer, T. P.; Kennedy, B. M.; Purtschert, R.; Severinghaus, J. P.; Solomon, D. K.; Tanhua, T.; Yokochi, R. 2014. Tracer Applications of Noble Gas Radionuclides in the Geosciences. *Earth-Science Reviews* **,** *138*, 196-214.

Mayer, A.; Sültenfuß, J.; Travi, Y.; Rebeix, R.; Purtschert, R.; Claude, C.; Le Gal La Salle, C.; Miche, H.; Conchetto, E. 2014. A multi-tracer study of groundwater origin and transit-time in the aquifers of the Venice region (Italy). *Appl. Geochem.*, doi:10.1016.

Melloul, A. J.; Zeitoun, D. G. 1999. A semi-empirical approach to intrusion monitoring in Israeli coastal aquifer. In *Seawater Intrusion in Coastal Aquifers – Concepts, Methods and Practices*; Bear J. et al., Eds.; Kluwer Academic Publishers: The Netherlands; pp 543-558.

Mercado, A. 1985. The use of hydrogeochemical patterns in carbonate sand and sandstone aquifers to identify intrusion and flushing of saline water. *Ground Water***,** *23*, 635-645.

Mook, W. G. 1980. Carbon-14 in hydrogeological studies. In *Handbook of Environmental Isotope Geochemistry, Vol. 1, The Terrestrial Environment*; Fritz, P., Fontes, J. Ch., Eds.; Elsevier Scientific Publishers: New York; pp 49-74.

Morrissey, S. K.; Clar,k J. F.; Bennett, M.; Richardson, E.; Stute, M. 2010. Groundwater reorganization in the Floridan aquifer following Holocene sea-level rise. *Nature Geoscience, 3*, 683-687; DOI:10.1038.

Paster, A.; Dagan, G.; Guttman, J. 2006. The salt-water body in the Northern part of Yarkon-Taninim aquifer: Field data analysis, conceptual model and prediction. *J. Hydrology***,** *323*, 154-167.

Purtschert, R.; Loosli, H. H.; Corcho, J. A. 2004. *How reliable are 39Ar ages?;* International Workshop on the Application of Isotope Techniques in Hydrological and Environmental Studies, UNESCO, Paris.

Purtschert, R.; Althaus, R. 2012. *Ar-39 dating of groundwater: How limiting is underground production?* Goldschmidt Conference; Montreal.

Purtschert, R.; Sturchio, N. C.; Yokochi, R. 2013. Krypton-81 dating of old groundwater. In *Isotope methods for dating old groundwater*; eds Suckow, A., Aggarwal, P., Araguas-Araguas, L., Eds.; IAEA : Vienna; pp 91-124.

Riedmann, R.; Purtschert, R. 2016. Separation of argon from environmental samples for Ar-37 and Ar-39 analyses. *Separation and Purification Technology*, 170 DOI: 10.1016/j.seppur.2016.06.017.

Rosenthal, E.; Weinberger, G.; Kronfeld, J. 1999. Groundwater salinization caused by residual Neogene and Pliocene sea water: an example from the Judea Group Aquifer, Southern Israel. *Groundwater***,** *37* (2), 261-270.

Russak, A.; Sivan, O.; Yechieli, Y. 2016. Trace elements (Li, B, Mn and Ba) as sensitive indicators for salinization and freshening events in coastal aquifers. *Chemical Geology*, DOI: 10.1016/j.chemgeo.2016.08.003.

Sanford, W. E. 1997. Correcting for diffusion in carbon-14 dating of groundwater. *Groundwater***,** *35*, 357-361.

Shachnai, E. 1980. *Yarqon-Taninim-Be'er Sheva basin, updating the hydrogeological model;* Rep. 01/80/12; Tahal Ltd., Tel Aviv, Israel, (in Hebrew).

Sivan, O.; Yechieli, Y.; Herut, B.; Lazar, B. 2005. Geochemical evolution and timescale of seawater intrusion into the coastal aquifer of Israel. *Geochim Cosmochim Acta***,** *69*, 579-592.

Sültenfuß, J.; Rhein, M.; Roether, W. 2009. The Bremen Mass Spectrometric Facility for the measurement of helium isotopes, neon, and tritium in water. *Isotopes in Environmental and Health Studies***,** *45* (2), 1-13.

Visser, A.; Broers, H. P.; Purtschert, R.; Sültenfuß, J.; de Jonge, M. 2013. Groundwater age distributions at a public drinking water supply well field derived from multiple age tracers (85Kr, 3H/3He, and 39Ar). *Water Resources Research***,** *49*, 7778-7796.

Weinberger, G.; Rosenthal, E.; Ben-Zvi, A.; Zeitoun, D. G. 1994. The Yarqon-Taninim groundwater basin, Israel hydrogeology: case study and critical review. *J. Hydrology* **,** *161*, 227–255.

Weiss, R. F. 1971. The effect of salinity on the solubility of argon in seawater. *Deep-Sea Res.*, *18*, 225-230.

Weiss, R. F.; Kyser, T. K. 1978. Solubility of krypton in water and seawater. *J. Chem. Eng. Data***,** *23* (1), 69-72.

Yechieli, Y.; Sivan, O.; Lazar, B.; Vengosh, A.; Ronen, D.; Herut, B. 2001. Radiocarbon in seawater intruding into the Israeli Mediterranean coastal aquifer. *Radiocarbon***,** *43*, 773-781.

Yechieli, Y.; Kafri, U,; Sivan, O. 2009. The inter-relationship between coastal sub-aquifers and the Mediterranean Sea, deduced from radioactive isotopes analysis. *Hydrogeol J.***,** *17*, 265-274.

Yokochi, R. 2016. Recent developments on field gas extraction and sample preparation methods for radiokrypton dating of groundwater. *Journal of Hydrology* **,** *540*, 368-378.

Table 1: Chemical and isotopic data of the water samples

field data and technical details

name of well	sampling date	EC millimho	DO mg/l	filter upper m	filter lower m	well alltitude masl	temp	pH	recharge temp celsius
Menashe T/3	2.6.14	54.2	0	978	1106	19	26.9	7.4	20
Gaash 1	2.6.14	40.5	0	841	1115	31	26.5	7.0	20
Gaash 2	2.6.14	53.0	0	1450	1750	31	26.4	7.8	20
Bet Eliezer deep	15.11.15	40.0	0	1087	1200	36	27.0	6.9	20
Raanana Deep	15.11.15	45.0	0	1154	1386	53	27.0	7.1	20
Taninim 7	15.11.15	45.0	0	505	645	7	27.8	7.2	20

general chemistry **stable isotopes**

name of well	Na^{+} mg/L	K^{+} mg/L	Ca^{++} mg/L	Mg^{++} mg/L	Cl^{-} mg/L	SO4 mg/L	HCO3 mg/L	TDS # mg/L	O-18 ‰	C-13 water ‰
Menashe T/3	12100	525	856	1210	21730	2865	276	39635	0.99	
Gaash 1	9270	240	358	462	15380	173	386	26327	-1.08	
Gaash 2	11320	453	1112	1158	21175	2645	185	38120	0.62	
Bet Eliezer deep	9453	258	1107	1224	18515	2296	206	33008	0.09	-9.6
Raanana Deep	10525	335	1184	1249	20240	2546	192	36228	0.63	-6.6
Taninim 7	9169	245	1221	1277	18742	1962	143	32686	0.02	-5.9
Mediter. seawater	12167	450	441	1482	22371	2928	165	40131	1.5	0

radiogenic isotopes

name of well	C-14 water pMC	Ar-39 % modern	error	Kr85 dpm/ ccKr	Kr81 partial modern	error	tritium measured TU	error	helium He3[ccSTP/kg]	helium He4[ccSTP/kg]
Menashe T/3				<0.55	1.1	0.05				
Gaash 1										
Gaash 2				<0.4	0.99	0.04				
Bet Eliezer deep	5.3	27	6	<0.69	0.94	0.03	0.36	0.04	5.61E-09	3.66E-03
Raanana Deep	3.6	22	11	<0.5	1.0	0.03	0.01	0.02	6.43E-09	4.71E-03
Taninim 7	2.9	10	<10	<0.66	1.02	0.04	0.05	0.03	5.18E-09	3.64E-03
seawater (current)*	105	100			1.0		1.50			

*** these values are the current surface sea values.**

Table 2. Estimated ages of the saline and fresh water components, calculated by the ^{81}Kr and ^{39}Ar dating methods.

Sample		Age young fresh (yr)			Age old saline (ka)	
	minimum	mean	maximal	minimum	mean	maximal
Bet Eliezier deep (BE)	30	100	200	13	26.5	40
Raanana Deep (RD)	50	950	1800	0.4	6.5	13
Taninim deep 7 (T7)	250	4700	9400	0.9	6.5	13

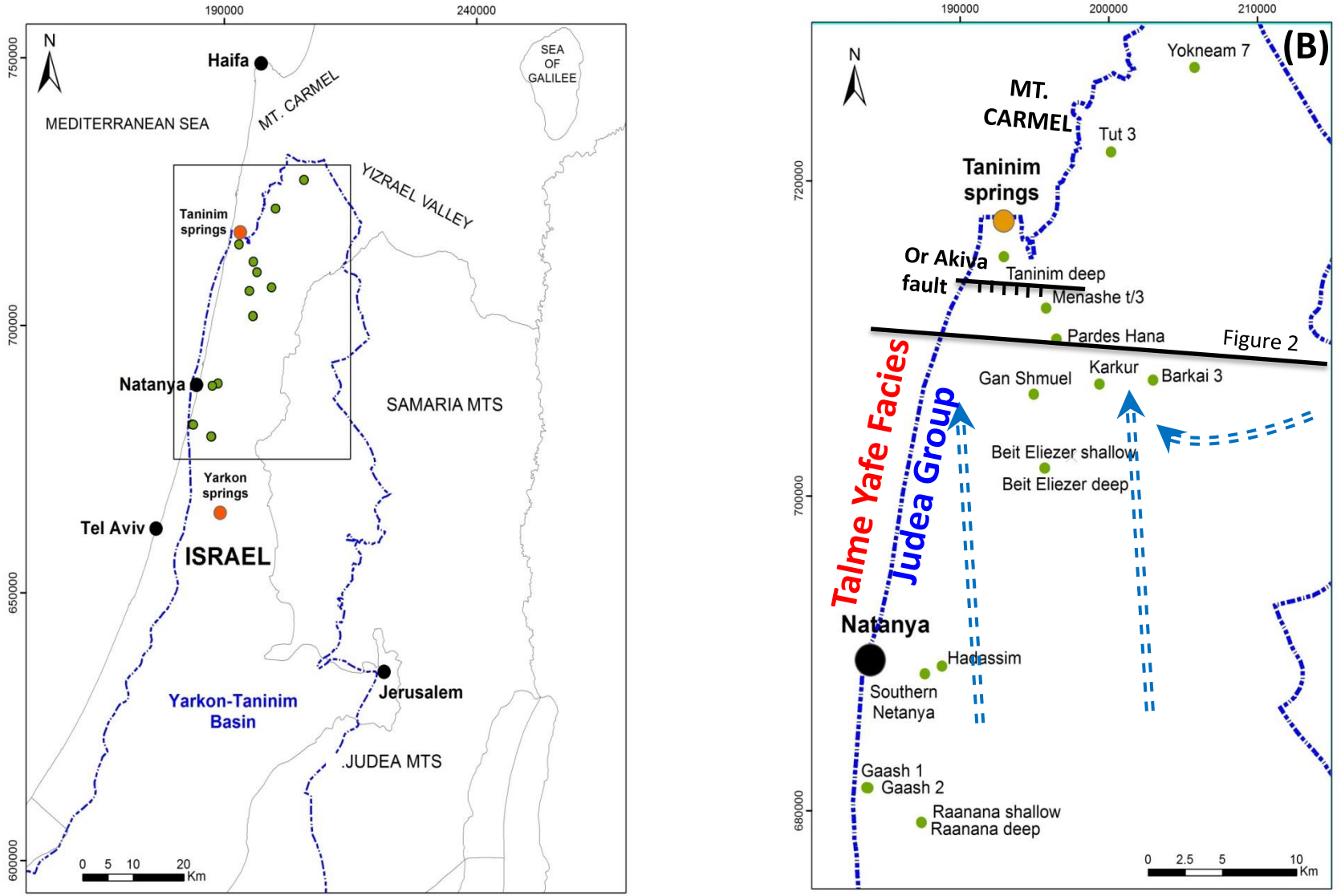

Fig. 1. Location map of the western Mountain aquifer (Yarkon-Taninim Basin - YTB) and the sampled wells. Blue arrows denote main directions of fresh groundwater flow. The southern part of the aquifer (Sinai and northern Negev) is outside the chart. Note the black line which denotes the western boundary of the YTB Aquifer with the impermeable TalmeYafe group.

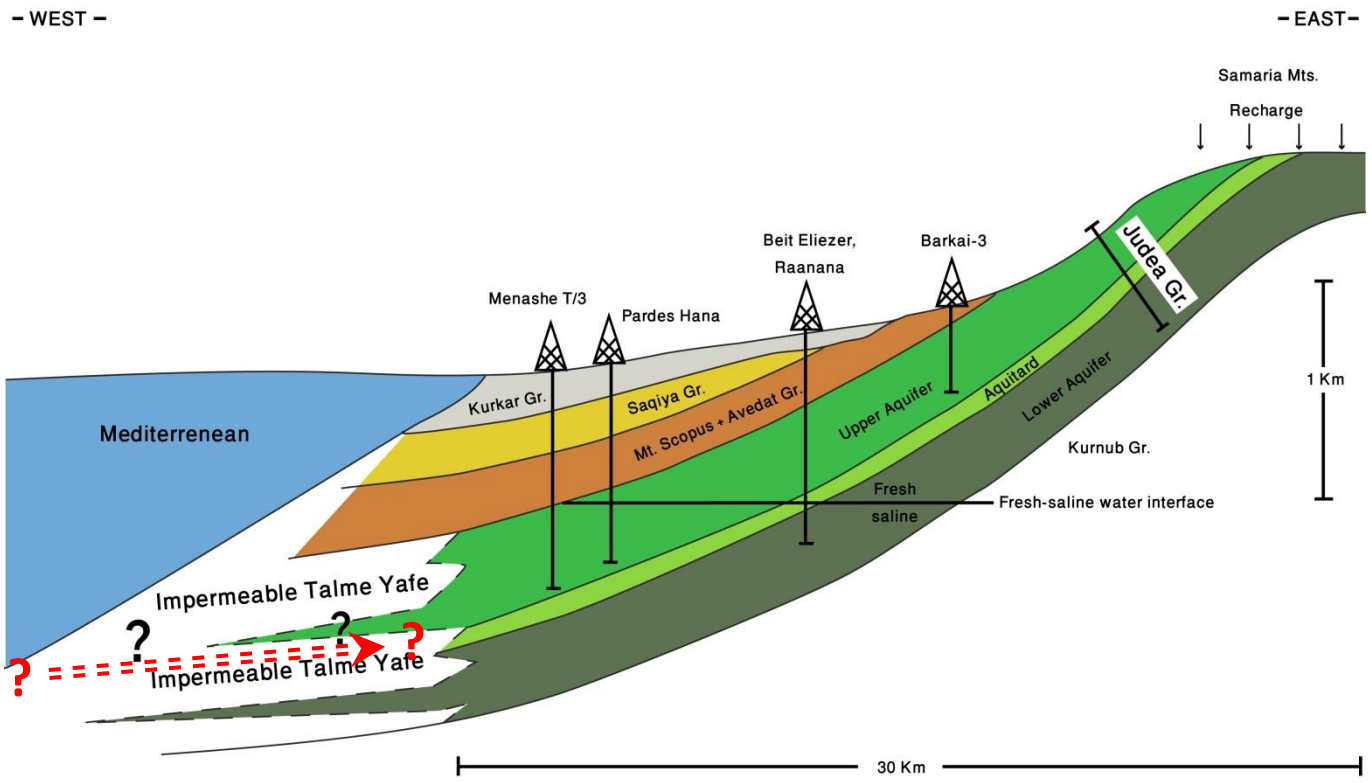

Fig. 2. Schematic cross-section from the Samaria Mountains in the east to the Mediterranean Sea in the west (see location in Figure 1). Some of the wells are projected onto the cross-section. The fresh-saline water interface is very close to be horizontal. The red broken line denotes possible seawater intrusion from the sea through openings in the TalmeYafe group.

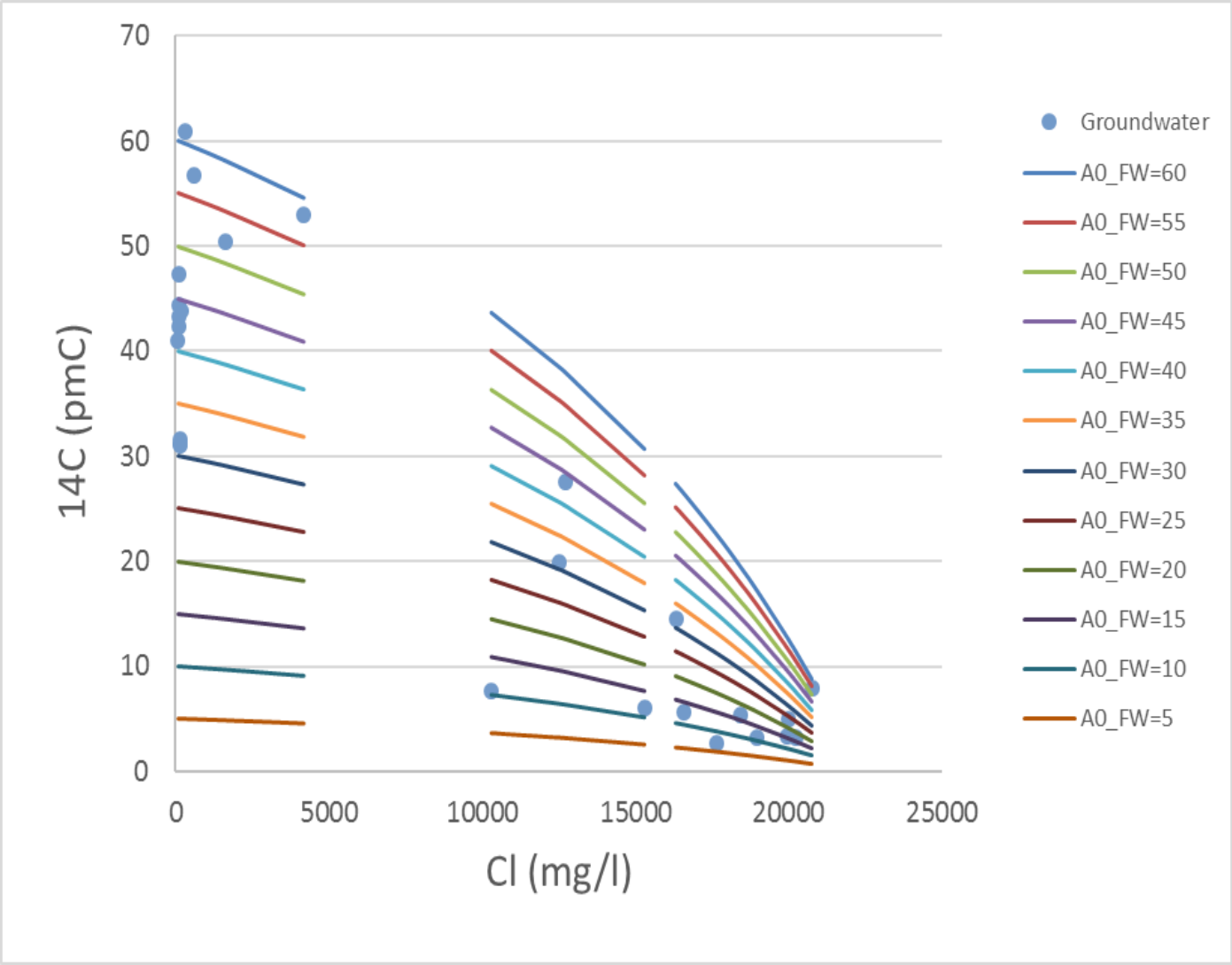

Fig. 3. Radiocarbon versus Cl concentration, showing the values in groundwater (blue points) in the studied area and also the possible values of the fresh and saline end member. The Colored lines are mixing lines according to different values of the initial concentration (A0) of the fresh water component. Data from Table 1 and from Burg et al. (2006) and Burg and Talhami (2013)

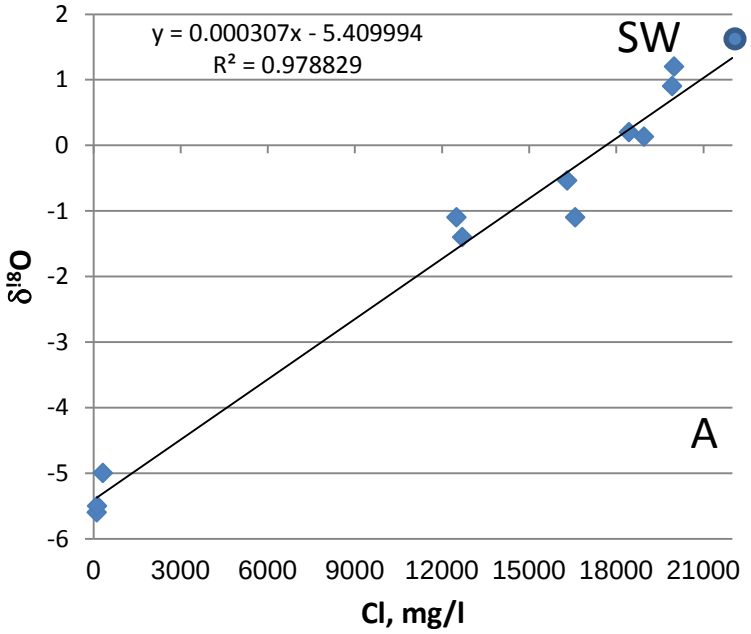

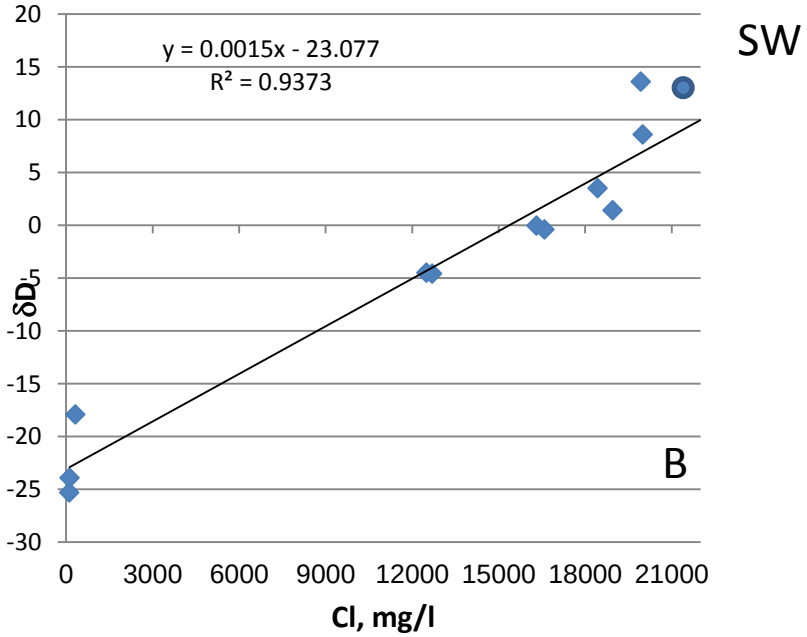

Fig. 4. d^{18}O and dD versus Cl concentrations, showing simple mixing line of fresh water with seawater, implying one source of saline water. Data from Table 1 and from previous studies (Burg and Talhami, 2013, Burg et al.,2006.

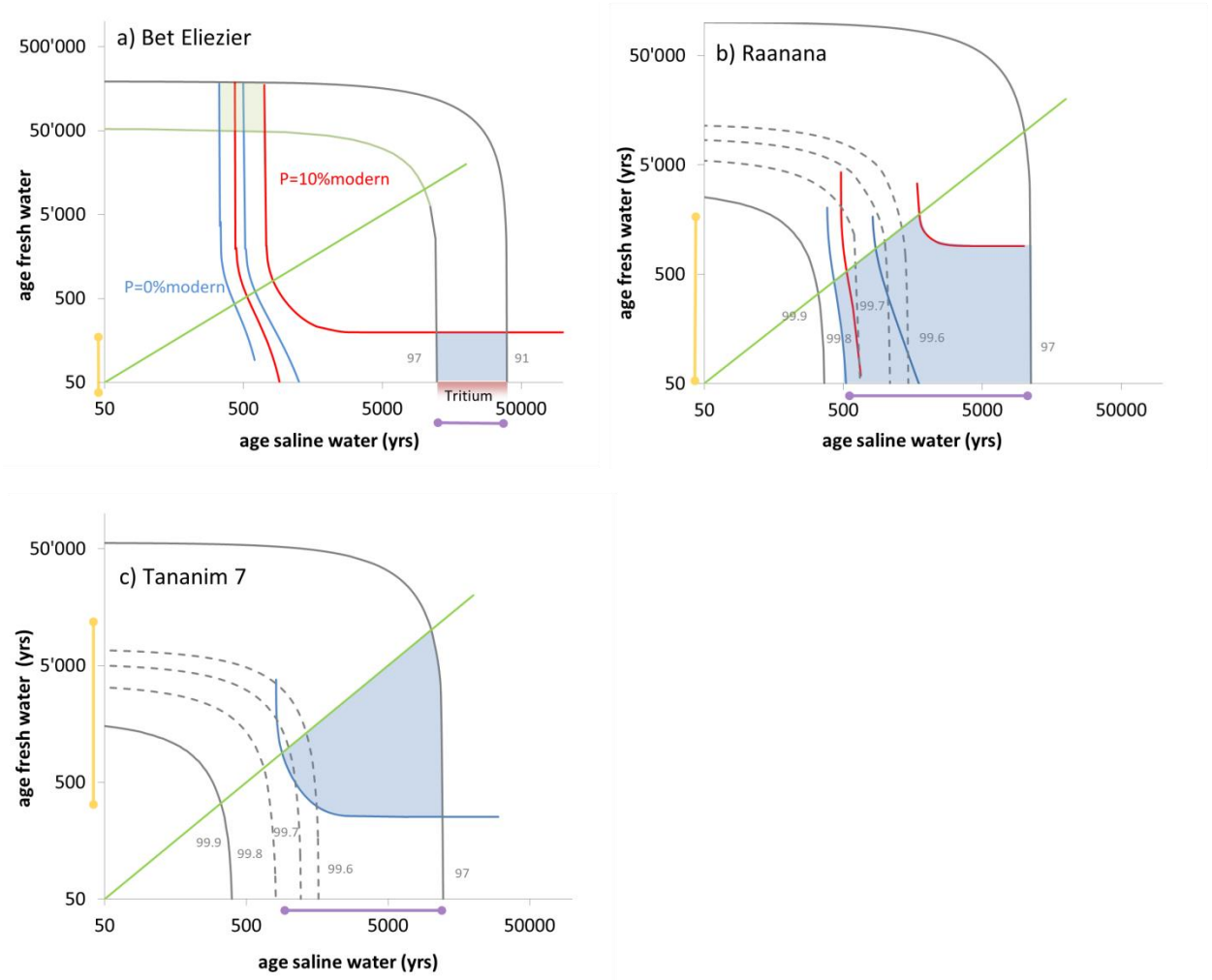

Fig: 5: Ages of saline and fresh groundwater. The blue area indicates possible age ranges in the t_f-t_s space. The red and blue lines define constrains from the ^{39}Ar data including the analytical uncertainties and a range for underground production from 0% modern (blue) and 10% modern (red). The grey curves provide the relation between t_f and t_s constrained by the ^{81}Kr data within uncertainties (grey labels; between the 1 s uncertainty range (68% confidence limit); if the measured $^{81}Kr/Kr$ ratio is >1 lower and upper values of 0.97 and 1 are assumed). The green line defines t_f=t_s. The resulting age bands for the fresh (orange) and saline water (violet) are also indicated.

Appendix

Table S1. Estimation of the percentage of the seawater component in the saline samples and the best fit of the initial value for the fresh water component (A_0). The last 3 samples are from the present work and the previous data are from Burg et al. (24) and Burg and Talhami (25). Maximal error of ^{14}C is 0.4 pmC.

ID	Name	Cl	f_saline	HCO_3	^{14}C	A_0_fw best fit
		mg/L		mg/L	pmC	pmC
22715501	Yokneam 7	16317	0.73	482	14.5	32
18813701	Netanya-south	16590	0.74	122	5.6	13
21514203	Taninim deep	17654	0.79	168	2.7	7
20114502	Bet Eliezier deep	18440	0.82	205	5.3	16
21514203	Taninim deep	18742	0.84	173	3.2	11
17913703	Ra'anana deep	19930	0.89	186	3.3	15
21114503	Menashe tav-3	20000	0.90	150	5.0	24
18113309	Ga'ash 2	20240	0.91	127	3.2	16
21114503	Menashe tav-3	20760	0.93	159	7.9	54
	Bet Eliezier deep	18515	0.83	206	5.3	16-30
This work						
	Raanana Deep	20240	0.91	192	3.6	11-20
This work						
	Taninim 7	18742	0.84	143	2.9	9-16
This work						

Table S2. The estimated ^{14}C ages of saline groundwater samples, using the inverse modeling of PHRREQC and NETPATH codes.

	Bet Eliezier	Ra'anana	Menashe t/3	Gaash 2
Seawater fraction	0.791	0.878	0.941	0.913
Calcite dissolution	3.29E-03	1.99E-03	-8.24E-04	2.65E-03
Dolomite dissolution	-1.64E-03	-9.67E-04	8.25E-04	-1.28E-03
CO2(g) production	3.20E-04	2.59E-04	1.00E-03	-2.06E-04
Na desorption	-5.01E-02	-5.39E-02	-2.25E-02	-3.49E-02
Mg desorption	9.03E-03	8.11E-03	0	0
Ca desorption	1.60E-02	1.88E-02	9.37E-03	1.58E-02
K desorption	0	0	3.79E-03	3.29E-03
H2S(g) production	0	0	0	7.90E-06
Age (PHREEQC)	21207	25412	22564	26750
Age (NETPATH)		23764	22012	

The codes calculated the seawater fractions in the saline groundwater, and the mass transfers (moles) of the different chemical processes. The estimation of the effect of these processes is essential for determination of the initial carbon values for the age calculation according to the radiocarbon decay equation. The main processes are ion exchange (mainly Ca versus Na) and Ca and Mg dissolution due to dissolution of rock-forming minerals. Another process that might affect is the CO_2 addition due to oxidation of organic matter upon the penetration of the seawater through the bottom sea sediment and into the aquifer. It should be noted that the age estimation is done for the saline samples, which are a mixture of sea water and fresh recharged water, and not for each component separately, and therefore should be regarded as an approximation. This was done because of the inability to estimate the specific initial values of the chemical and isotopic parameters in each component (seawater and fresh groundwater). However, since the saline sample is dominated by the seawater fraction, the age of penetrating seawater can be regarded as well estimated by this calculation (even though the bicarbonate concentration in fresh groundwater is about double that of seawater). The temperature of seawater at the relevant depth (~1000m) is about 14^0C and the ambient temperature of the fresh water component at the recharge zone is about 20^0C. Therefore, the relevant temperature for the calculation in this study is something in between these two values.

NETPATH model did not produce ages for Bet Eliezier and Gaash2 wells, probably due to inaccuracy in some of the chemical parameters which lead to numerical problems in running these specific simulations. For these wells, only the results of the PHREEQC are given.